Development of high-repetition-rate laser pump/x-ray probe methodologies for synchrotron facilities

Anne Marie March, Andrew Stickrath, Gilles Doumy, Elliot P. Kanter, Bertold Krässig, Stephen H. Southworth, Klaus Attenkofer, Charles A. Kurtz, Lin X. Chen, and Linda Young

---

Development of high-repetition-rate laser pump/x-ray probe methodologies for synchrotron facilities

Anne Marie March,[1,a)] Andrew Stickrath,[2] Gilles Doumy,[1] Elliot P. Kanter,[1] Bertold Krässig,[1] Stephen H. Southworth,[1] Klaus Attenkofer,[1] Charles A. Kurtz,[1] Lin X. Chen,[2,3] and Linda Young[1]

[1]*X-ray Science Division, Advanced Photon Source, Argonne National Laboratory, 9700 S. Cass Ave., Argonne, Illinois 60439, USA*
[2]*Chemical Sciences and Engineering Division, Argonne National Laboratory, 9700 S. Cass Ave., Argonne, Illinois 60439, USA*
[3]*Department of Chemistry, Northwestern University, 2145 Sheridan Road, Evanston, Illinois 60208, USA*

We describe our implementation of a high repetition rate (54 kHz–6.5 MHz), high power (>10 W), laser system at the 7ID beamline at the Advanced Photon Source for laser pump/x-ray probe studies of optically driven molecular processes. Laser pulses at 1.06 μm wavelength and variable duration (10 or 130 ps) are synchronized to the storage ring rf signal to a precision of $\sim$250 fs rms. Frequency doubling and tripling of the laser radiation using nonlinear optical techniques have been applied to generate 532 and 355 nm light. We demonstrate that by combining a microfocused x-ray probe with focused optical laser radiation the requisite fluence (with <10 μJ/pulse) for efficient optical excitation can be readily achieved with a compact and commercial laser system at megahertz repetition rates. We present results showing the time-evolution of near-edge x-ray spectra of a well-studied, laser-excited metalloporphyrin, Ni(II)-tetramesitylporphyrin. The use of high repetition rate, short pulse lasers as pump sources will dramatically enhance the duty cycle and efficiency in data acquisition and hence capabilities for laser-pump/x-ray probe studies of ultrafast structural dynamics at synchrotron sources. © *2011 American Institute of Physics*. [doi:10.1063/1.3615245]

I. INTRODUCTION

Ultrafast and time-resolved x-ray measurement techniques, which combine ultrafast lasers and short pulse x-rays in pump-probe experiments, are powerful tools for understanding and controlling the behavior of matter at the molecular level.[1–7] These techniques can offer sub-Ångstrom spatial resolution and temporal resolution down to the picosecond or femtosecond regimes. In addition, the elemental specificity and penetration power of x-rays can allow for *in situ* measurements of systems in complex or disordered environments.[2] While now there are a variety of short pulse x-ray sources available for these studies, including table-top sources based on high harmonic generation[8–10] or laser-induced plasmas[11–14] and large accelerator based facilities such as x-ray free electron lasers,[15] third generation synchrotron sources[16] such as the Advanced Photon Source (APS), provide a unique combination of x-ray properties that are particularly well suited for precision time-resolved measurements. These include tunability over a large x-ray energy range (several keV), stability ($<0.3\%$ fluctuations in average flux), defined polarization, high flux (10^{13} photons/second/0.01% bandwidth), and high pulse repetition rate (MHz).

In a typical laser/x-ray pump-probe experiment, a laser pulse excites a sample to create a transient, non-equilibrium state and an x-ray pulse follows, at a fixed time delay relative to the laser pulse, to probe the transient state. X-ray absorption, emission, diffraction, or scattering signals can be detected and signal is accumulated over many pump-probe cycles to satisfy the signal to noise ratio required for data analysis. This process can be repeated at different delays to map out the temporal behavior of the transient states. Successive x-ray pulses in the x-ray pulse train, between laser pump pulses, can also be used to probe the structural evolution of transient states on time scales longer than the picosecond range covered by individual pulses, allowing disparate time scales to be probed in the same experiment. The APS, in its standard operating mode, produces x-ray pulses with moderate flux (e.g., $\sim$10^6 photons/pulse in a monochromatized beam at 7ID) at a high repetition rate (6.52 MHz, 153 ns interbunch spacing), weak enough to act as nonperturbative probes but at a flux high enough to produce high quality data, even considering the inherently weak interaction of x-rays with matter (a typical x-ray absorption cross section is 10^{-5} times that in the visible regime). Also, the timing properties of the APS make it a particularly attractive synchrotron storage ring for timing studies; the long 153 ns interbunch spacing allows easily gateable detectors and mechanical choppers to select individual x-ray pulses and such timing modes are available 80% of the beamtime.

For several years, time-resolved x-ray/laser experiments have been carried out at synchrotrons. However, very few, if any, have been able to utilize the full x-ray flux available. While for some experiments this has been due to sample or detector constraints, for many experiments involving quickly replenishable or reversible systems the main limitation has been the repetition rate of the laser system. For experiments

a)Electronic mail: amarch@anl.gov.

requiring laser pulse energies greater than the nJ per pulse provided by laser oscillators, laser amplifiers are required. Standard solid state amplifiers, such as multipass and regenerative amplifiers, boost the laser pulse energy of ultrafast systems to ~1 mJ, but at a cost of the pulse repetition rate, typically reducing it from ~80 MHz in the oscillator to the range of 1–5 kHz where, with only a few exceptions,[17–19] experiments have been limited. This inefficient use of the available flux has led to dramatically longer data collection times than are required for steady-state experiments, limiting the number of parameters that can be explored in a given beamtime, or leading to data with poorer quality statistics. This limitation is particularly severe for studies of dilute samples, such as gas phase molecules[20,21] and low concentration solution phase molecules.

Advances in laser technology are now dramatically altering possibilities. In this paper we report on the implementation of a high repetition rate (54 kHz–6.5 MHz), high power (>10 W), laser system at the 7ID beamline at the APS. In order to utilize the highest repetition rate of the laser, where it has relatively meager per pulse energy (few μJ), it is essential to incorporate an x-ray microprobe geometry, as originally implemented on Sector 7 to study orbital dynamics in strong-field ionized atoms.[22] The experimental details of the laser system, including its synchronization with the x-rays, are included in Sec. II. Section III describes the details of a demonstration experiment where we carried out time-resolved x-ray absorption spectroscopy on a metalloporphyrin molecule in solution. Section IV includes the experimental results along with discussion. Section V concludes and presents an outlook for this experiment and of other high repetition rate experiments.

II. EXPERIMENTAL DETAILS

A. High repetition rate laser system

The high repetition rate laser is a customized commercial master oscillator power amplifier (Time-Bandwidth Products, Duetto) with a central wavelength of 1064 nm and a variable repetition frequency and pulse duration. The repetition frequency is selected by specifying the rate at which pulses from the oscillator train are picked for amplification. The oscillator repetition frequency was customized to be 78.2 MHz. The laser is designed to operate at all submultiples of the oscillator frequency between 54 kHz (78.2 MHz $\div$ 1440) and 6.52 MHz (78.2 MHz $\div$ 12). The system produces 10 W power at 54 kHz, corresponding to 185 μJ/pulse, and 16 W at 6.52 MHz, corresponding to 2.5 μJ/pulse. The laser can produce pulses with durations of either 10 ps FWHM or 130 ps FWHM. The 10 ps duration is useful for experiments requiring optical excitation of molecules[2,4] whereas the 130 ps duration is suitable for experiments with laser-dressed atoms or molecules[6,20] in conjunction with the presently available ~100 ps pulses from the APS. Switching between the two modes is easily accomplished by inserting or removing an etalon in the oscillator. The oscillator and power amplifiers are contained in a single, hermetically sealed, compact box, making the system practical for the small space and fluc-

tuating temperatures of an x-ray hutch and making it possible for the laser to be kept close to the experiment, providing the advantage of fewer transport optics and less loss of power in transport.

The second and third harmonics of the laser, at 532 nm and 355 nm, are generated by focusing the output into two lithium triborate nonlinear crystals (Newlight Photonics). The second harmonic is produced in a crystal with dimensions $5 \times 5 \times 15$ mm^3 that is cut for Type I mixing and non-critical phase matching. The crystal is held in a precision temperature stabilized oven (Newlight Photonics). Efficient second harmonic production occurs at a nominal temperature of 150 °C. The third harmonic is produced by mixing the second harmonic light at 532 nm and the residual fundamental light at 1064 nm in a $5 \times 5 \times 15$ mm^3 crystal that is cut for Type II mixing. Phase matching is achieved by angle-tuning the crystal. Because of the high power (~10 W) incident upon the crystal, heating can cause changes in the index of refraction that disrupt the mixing efficiency and produce unstable output power. To counteract that, this crystal is also held at an elevated temperature (~100 °C) in a precision temperature stabilized oven. In order to achieve high conversion efficiencies across the full range of repetition frequencies, where the energy per pulse varies by a factor of 75, we have implemented an optical system that allows us to change the laser spot size incident upon the second harmonic and third harmonic crystals by translating a lens within a telescope. We achieve high second harmonic conversion efficiencies (~80%) by maintaining an average incident intensity of 1.5 GW/cm^2 for all repetition rates between 54 kHz and 6.52 MHz. For the third harmonic, we achieve 1064 nm to 355 nm efficiencies of 35%–40%. See Table I for the pulse powers and energies we achieve.

The laser and any of its harmonics are easily focused to a spot size of 25 μm FWHM at the sample position, which produces an intensity of 1.3 TW/cm^2 (10 ps, 1064 nm) at 54 kHz and 18 GW/cm^2 (10 ps, 1064 nm) at 6.52 MHz. While this range of intensities is more than enough to saturate single photon excitations in molecules, for other experiments in the gas phase such as laser alignment[20] or laser dressing[21] 1 TW/cm^2 is typically a lower bound. Such experiments are limited to 54 kHz with the present laser and will need to await more powerful lasers to be carried out at higher repetition rates.

The laser fluence at the sample is controlled either by reducing the power, using an attenuator comprised of a waveplate and polarizer, or by adjusting the spot size at the sample. This is done by translating the focusing lens along the laser propagation axis.

TABLE I. Available power and pulse energy at the fundamental, second, and third harmonics in the 10 ps operational mode at selected repetition rates.

Wavelength	54.3 kHz		135.8 kHz		3.25 MHz		6.52 MHz	
	W	μJ	W	μJ	W	μJ	W	μJ
1064 nm	10	185	11.3	83	14.5	4.4	16	2.5
532 nm	7.0	130	8.9	66	10.6	3.3	9.5	1.5
355 nm	2.5	45	4.2	31	4.8	1.5	3.6	0.6

B. Synchronization and delay control

The high repetition rate laser can be synchronized to the x-rays produced in any of the storage ring operation modes used at the APS. Of these modes, the standard "24 bunch" operating mode and the "hybrid singlet" operating mode are particularly useful for pump-probe experiments. In the 24 bunch mode, 24 electron bunches evenly spaced by 153 ns circulate the storage ring at a revolution frequency of 272 kHz and with a total current of 102 mA. X-ray pulses are produced at a repetition rate of 6.52 MHz. Continuous "top-up" is run in this mode, where one of the bunches is refilled every two minutes, maintaining an average current stability over all 24 bunches of <0.3%. Each bunch contains a nominal current of 4.25 mA, which is "topped up", on average, every 48 min. The decay of a single bunch between top-ups can be as much as 15%, necessitating the use of a gated avalanche photodiode or other flux detector to monitor the time varying flux produced by selected electron bunches. The electron bunch length in this mode is 40 ps rms and the x-ray pulses have a similar duration.[23]

In the hybrid singlet mode, a single bunch, with 16 mA, circulates the ring at 272 kHz opposite a train of eight groups containing seven bunches each. The singlet is separated from the eight septuplets by 1.594 μs on each side. The total current in this mode is 102 mA. The 86 mA not contained in the singlet bunch is distributed among the septuplets. The spacing between bunches within a septuplet is small, only 2.8 ns, making it difficult to use these bunches for time resolved measurements, since the response time of commonly used detectors is too slow to resolve signal due to only one bunch. Because of this, these bunches are not used and only the singlet bunch is utilized for pump-probe experiments. Continuous top-up is run in this mode, with injection occurring at one minute intervals, leading to a stability in the singlet pulse of 3%–6%. The rms duration of the singlet bunch, and hence x-ray pulses, is 65 ps.[23]

Using traditional amplified laser systems ($\sim$1 kHz), a laser pulse would overlap only one out of every 6520 x-ray pulses in 24 bunch mode, limiting the usable x-ray flux to less than 0.1%, dramatically underutilizing the synchrotron's capabilities. In hybrid singlet mode, the laser pulse will overlap only every 272nd x-ray pulse from the singlet bunch. The high repetition rate laser can match the x-ray repetition rate in either of these modes and can also operate at submultiples of either mode which can be advantageous for some experiments where longer time scales are probed, larger laser pulse energy is needed, or sample recovery or replenishing time is a limiting factor.

Synchronization of the laser pulses with the x-ray pulses and control of the delay between the two is accomplished electronically and is depicted in Figure 1. The laser pulses are stabilized in time with respect to the x-ray pulses with a phase-lock-loop contained within a clock synchronizer feedback system (Time Bandwidth Products, CLX-1100). The oscillator cavity length is adjusted with a piezo-actuated cavity mirror mount to lock the oscillator pulse train repetition rate to the storage ring rf signal which has been down converted to 78.2 MHz from 352 MHz by an in-house built frequency
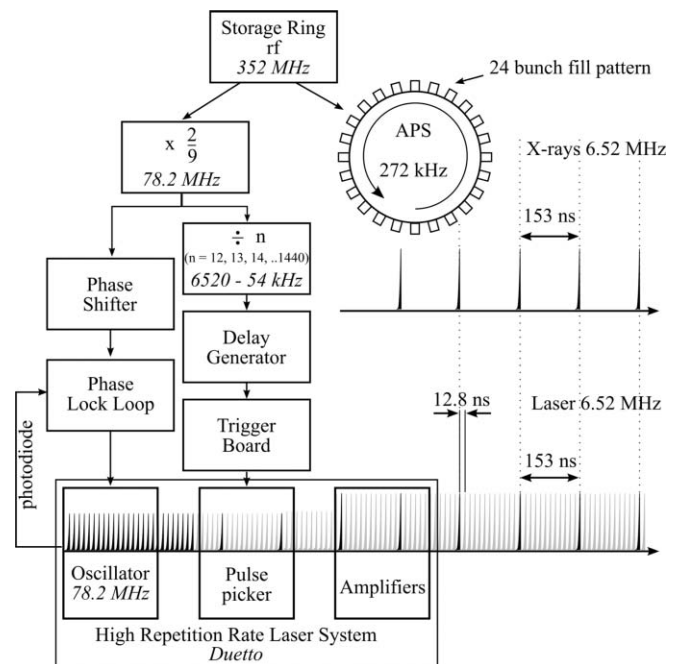

FIG. 1. Schematic of the synchronization and delay control of the laser pulses with respect to the x-ray pulses. The laser is shown operating at 6.52 MHz (78.2 MHz ÷ 12) to match the x-rays in the standard 24 bunch mode. The light gray pulses separated by 12.8 ns illustrate other oscillator pulses that could be chosen for coarse delay of the laser relative to the x-ray pulses.

divider that multiplies by 2 and then divides by 9. The locking bandwidth of the system is 100 kHz. The oscillator pulse-to-pulse timing jitter with respect to the down converted rf signal is stabilized to a precision of $\sim$250 fs rms. The trigger for the pulse picker within the laser is also derived from the 352 MHz storage ring rf signal. After downconversion by the 2/9 frequency divider, the signal is sent to another frequency divider with a variable integer divisor value (Pulse Research Lab, PRL-260BNT). Dip switches on this frequency divider set the divisor value. The divided signal is input into the custom made trigger board located in the laser controller, and drives the rf signal to the acoustic optic modulator within the laser which does the pulse picking of oscillator pulses for amplification. Changing the dip switches on the variable frequency divider is all that is required to change the laser repetition frequency and doing so does not disrupt the synchronization.

Control of the laser delay with respect to the x-ray pulse on target is implemented in two parts. Coarse temporal delay is achieved through the selection of particular laser pulses within the oscillator pulse train for amplification. By adding a delay in the trigger signal using a delay generator (SRS, DG645), later pulses of the oscillator pulse train are selected. Since the oscillator repetition frequency is 78.2 MHz, this effectively leads to control of the laser delay in 12.8 ns steps. Control of the fine delay is achieved by shifting the phase of the rf reference signal before the phase-lock-loop. This effectively shifts the oscillator pulse train in time. A programmable delay line (Gigabaudics, PADL3-5-12-15355) shifts the reference signal in steps of 5 ps, with a range of 15 ns.

C. X-ray microprobe

The Duetto laser is located at Sector 7 in the 7ID-D hutch at APS. Details of the 7ID APS Type-A undulator beamline have been described elsewhere.[24] The main points will be highlighted here. A water-cooled double crystal diamond (111) monochromator (Kohzu, HLD4) with energy bandpass FWHM $\delta E/E = 5.4 \times 10^{-5}$ is capable of tuning the energy from 5.2 keV to 24 keV, using the first and third undulator harmonics. The x-ray flux after the monochromator is $\sim 10^{12}$–10^{13} photons/s, corresponding to $\sim 10^5$–10^6 photons/pulse in the 24 bunch operational mode. Kirkpatrick-Baez mirrors (Instrument Design Technology)[25] focus the x-ray beam to a spot size of $\sim 5 \mu$m FWHM at the sample location and deliver $\sim 2 \times 10^{12}$ photons/second on target at 10 keV.

The microfocused x-ray beam provides several advantages. By keeping the x-ray spot smaller than the laser spot, one probes a region of more uniform intensity and efficient optical excitation. Most importantly, the small spot sizes (x-ray < 10 μm, laser ~ 25–50 μm) allow the fluence available from compact, megahertz repetition rate lasers to saturate optical transitions. Also, a small x-ray spot allows one to have a small laser spot, which limits the laser power incident upon the sample for a given laser fluence, reducing detrimental effects such as heating. In addition, for flowing samples, smaller spots reduce the time required for molecules to leave the interaction region to generate a fresh sample for subsequent pulses.

D. Spatial and temporal overlap

To spatially overlap the laser and x-ray beams, a pinhole or knife edge is positioned in place of the sample and scanned horizontally and vertically in the plane perpendicular to the laser and x-ray beam propagation direction while the transmitted laser power is monitored on a power meter and the transmitted x-ray power is monitored on an ion chamber. The pin hole is first centered on the x-ray beam, and then the horizontal and vertical positions of the laser focusing lens are adjusted to center the laser on the pin hole.

To maintain the spatial overlap over long time periods, a laser beam stabilization system is employed (MRC Systems). This compensates for drifts of the laser pointing and maintains the position of the laser on the sample to within 5 μm. This position at the sample, as well as the laser spot size are monitored on a CCD camera that detects the leakage through the last turning mirror before the sample.

To temporally overlap the laser and x-ray pulses, an MSM photodetector (Hammamatsu, G4176-03), with a rise time of 30 ps, is positioned in place of the sample. The x-ray beam and attenuated laser beam are shone on the detector. Pulses from each beam are observed on a single trace using a 3.5 GHz, 40 Gs/s digital oscilloscope (LeCroy, Wave-Pro 735Zi). The delay of the laser pulses is adjusted electronically to overlap the laser pulses and x-ray pulses in time, to an estimated precision of ± 10 ps. The temporal overlap can then be precisely determined by cross correlation of the laser and x-rays monitoring an experimental feature, e.g., a laser-induced feature in the x-ray absorption spectrum. The spatial overlap can also be optimized by monitoring the sample response.

III. X-RAY ABSORPTION SPECTROSCOPY DEMONSTRATION EXPERIMENT

As a demonstration of the high repetition rate laser's capabilities we carried out a time resolved x-ray absorption spectroscopy (XAS) experiment[2,3,26–28] on a transient laser excited state of Ni(II)-tetramesitylporphyrin (NiTMP) in a 2 mM toluene solution. NiTMP is a model system for the class of molecules called metalloporphyrins, which constitute the active center of biologically relevant molecules such as chlorophylls and heme groups. This system has been studied in depth[29–31] and was chosen as a test case because of its known rich features in both the x-ray absorption near-edge structure (XANES) and x-ray absorption fine structure (XAFS) regions that are relevant to its complicated photo-chemistry as well as its known robustness under prolonged exposure to both laser and x-ray. It consists of a nickel atom situated within a porphyrin ring.[29] Upon laser excitation with 532 nm light, an electron is promoted through a π to π^* transition involving orbitals with predominantly porphyrin macro-cycle character. This short-lived excited state undergoes an intramolecular energy transfer (within 350 fs) to a Ni(II)-centered state which vibrationally relaxes (within 20 ps) to a longer lived Ni(II)-centered presumably triplet state, T_1. The T_1 state decays back to the ground state in about 200 ps. The Ni(II) ($3d^8$) electronic configuration of the T_1 excited state differs from the ground state in that it has half filled $3d_{x^2-y^2}$ and $3d_{z^2}$ orbitals while the ground state has an unfilled $3d_{x^2-y^2}$ orbital and a doubly occupied $3d_{z^2}$ orbital. Due to the x-ray pulse duration (40 ps rms), the fast intramolecular energy transfer and vibrational relaxation intermediate states cannot be resolved and hence it is only the T_1 state that is predominantly probed. The system is an example of how electronic redistribution leads to molecular geometry rearrangements. The promotion of the electron to the antibonding $3d_{x^2-y^2}$ orbital at the Ni atom leads to an expansion of the porphyrin ring.[29]

The experiment was carried out using the standard 24 bunch mode and the second harmonic of the Duetto laser system, at 532 nm, in the 10 ps (FWHM) mode of operation. The laser repetition rate was 135.8 kHz, so that one x-ray pulse out of every 48 probed a laser excited sample. Given the fast decay time of the excited state (200 ps) relative to the time between successive x-ray pulses (153 ns), all 47 of the x-ray pulses between the laser pulses probed the ground state of the molecule. This allowed for the ground state and laser excited state absorption spectra to be collected within the same scan, which was important to ensure the energy calibration between the two spectra.[29] Also, changes in the ground state spectrum could indicate possible sample degradation. This laser repetition rate was chosen so that a fresh volume of the sample within a flowing liquid jet would be present for each laser shot, given the liquid flow rate of ~ 5 m/s. This repetition rate is also important for experiments done in hybrid singlet mode, as it allows for all of the singlet x-ray pulses, which arrive at 272 kHz, to be used, with half of the pulses probing the excited state and half probing the ground state.
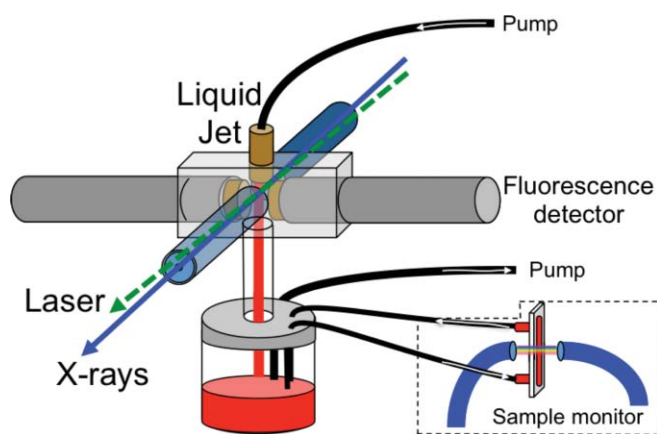
FIG. 2. (Color online) Experimental arrangement for the time-resolved XAS measurement of NiTMP in toluene.

A. Liquid jet apparatus

Figure 2 depicts the setup for the XAS measurement. The liquid jet was housed in an enclosed assembly that is adaptable for different detectors and jets and that can be purged with nitrogen or other gases to, for example, protect oxygen sensitive samples. The sample (2 mM NiTMP in toluene) flowed through a sapphire nozzle in a flat liquid jet with thickness $\sim$100 μm and width of $\sim$6 mm and that was oriented 45° relative to the beams. The flow speed was $\sim$5 m/s. The laser entered and exited the enclosure through fused silica windows that were held by 12 in. long tubes, away from the jet to prevent liquid from reaching the window surfaces and far enough for the laser and x-ray beams to be spatially separated from each other. The x-ray beam entered and exited through holes in the centers of the windows which were sealed with kapton tape. The laser and x-ray beams intersected at the position of the jet, with a small crossing angle of $\sim$2°. An f/16 AR coated fused silica lens focused the laser, producing a FWHM spot size of $\sim$60 $\times$ 60 μm^2 at the liquid jet sample. For this experiment the x-rays were focused to a FWHM spot size of 10×20 μm^2. The integrity of the sample can be monitored during the experiment by continuous measurement of the visible absorption spectrum. The sample is sent through a flow cell through which the transmission of a white light source (Ocean Optics, HL2000) is monitored on a small spectrometer (Ocean Optics, HR2000+CG).

Unresolved Ni $K\alpha$ and $K\beta$ fluorescence (7.478 keV and 7.460 keV) was detected by an avalanche photodiode (APD) (Perkin Elmer, C30703F) with a detection area of 10×10 mm^2. The number of molecules in the probed region was small ($\sim$1.2 $\times$ 10^{10}) and so the number of detected fluorescence photons per x-ray pulse was low ($\sim$0.02 counts/pulse above the K edge). This allowed for the APD to be operated in pulse-counting mode. The APD was positioned to collect photons emitted orthogonally to the laser and x-ray propagation direction and along the x-ray polarization direction to minimize detection of scattered x-rays. A soller slit spatial filter and $Z - 1$ (cobalt) filter positioned before the APD removed background from elastic and inelastic scatter-

ing. The x-ray fluorescence and scattered x-ray spectrum was measured with a silicon drift detector and confirmed that fluorescence was the dominant component detected. Aluminized mylar foil was used to block the scattered laser radiation from the APD. A single detector was used, although the setup allows for two detectors, positioned on each side of the liquid jet as indicated in Figure 2.

B. Data acquisition

A time-resolved XAS spectrum was collected by setting the delay between the laser pulse and x-ray pulse to a fixed value and scanning the incident x-ray photon energy across the Ni K edge (8.333 keV). At each photon energy step, fluorescence counts were tallied. Because the response of the APD is fast (5 ns) compared to the separation between x-ray pulses (153 ns), counts from an individual x-ray pulse can be distinguished using gate/delay units in the data acquisition system. By sending the discriminated output of the APD through a logic circuit, along with gate pulses that are synchronized with the lasers and x-ray pulses, counts originating from x-ray pulses that probe the laser excited sample are tallied independently from counts originating from x-ray pulses that probe the ground state. The relative timing of the gate, x-ray, and laser pulses is shown in Figure 3. The laser gate selects the x-ray pulses that are overlapped with the laser and the singlet gate selects all x-ray pulses originating from the electron bunch that produces laser-overlapped x-ray pulses. Counts that are not concurrent with the laser gate generate the ground state spectrum. Counts that are concurrent with the laser gate and counts that are concurrent with the singlet gate, but not the laser gate are used to construct a laser-on/laser-off ratio. By using this ratio to detect changes in the fluorescence signal from the laser excited state, many systematic errors can be eliminated since consecutive x-ray pulses from the same electron bunch have similar characteristics. The laser excited spectrum is then generated by multiplying this ratio by the ground state spectrum.
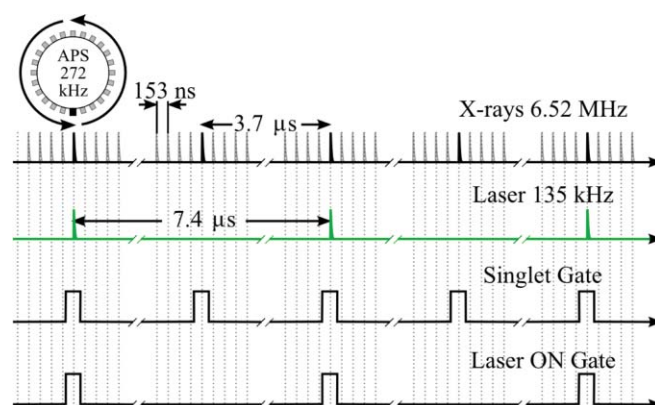

FIG. 3. (Color online) Data acquisition scheme using a single 4.2 mA bunch to record laser-on/laser-off data at 135 kHz. Electronic gates are used to distinguish counts from x-ray pulses from a selected bunch and also those from x-ray pulses that are overlapped with the laser pulses.
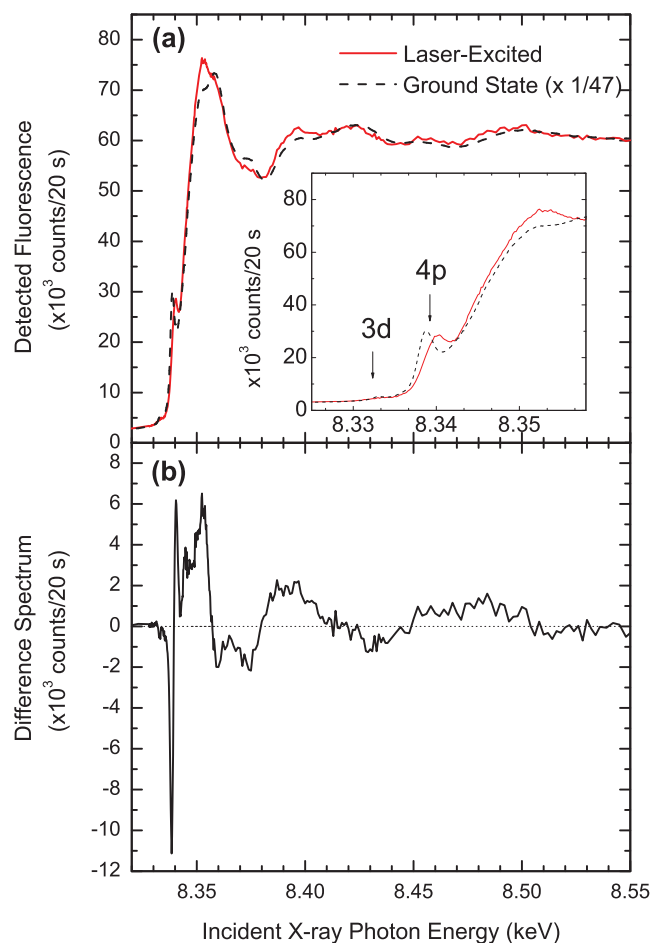
FIG. 4. (Color online) (a) XAS fluorescence yield at the Ni K edge from NiTMP solvated in toluene, collected in a single scan in one hour. Shown are the laser excited (solid curve) and ground state (dashed curve) spectra. The ground state spectrum was collected from all x-ray pulses but the laser-on and so has been divided by 47 to be compared with the laser excited spectrum. The laser repetition rate was 135.8 kHz. The x-rays probed 50 ps after the laser pulse. The laser power was 0.7 W corresponding to 5 μJ/pulse. The inset shows the $1s \rightarrow 4p$ and $1s \rightarrow 3d$ edge features. (b) Difference spectrum between the laser excited and ground state spectra shown in the top panel.

IV. RESULTS AND DISCUSSION

Figure 4 shows the ground state and laser excited state absorption spectra from one scan where 194 energy steps were taken with an integration time of 20 s at each point. The scan took approximately one hour to collect. As can be seen in the difference spectrum in the bottom panel in Figure 4, even with a single shot fluorescence count rate (above the edge) of 0.023 counts/pulse, a laser excited spectrum exhibiting clear changes from the ground state spectrum can be obtained in a reasonable amount of time. By comparison, at 1 kHz and with a similar count rate, the same measurement would have taken 147 h.

The inset shows the distinctive edge resonance feature which corresponds to the $1s \rightarrow 4p_z$ transition.[31] In the ground state molecule, this resonance occurs at 8.338 keV. In the T_1 state, it is shifted to higher energy by 1.5 eV.[29,31] This shift is easily seen in the laser excited absorption spectrum, which contains contributions from both the T_1 state and the ground state, indicating that the fraction of T_1 state molecules

in the probed region is high. To obtain an estimate for the excited state fraction in our experiment, we fit the $1s \rightarrow 4p_z$ resonance region in the laser excited spectrum with two Gaussian peaks, one at the ground state position derived from the measured ground state spectrum (8.3387 keV) and the other 1.5 eV higher (8.3402 keV). The widths of the peaks were fixed to match the width from the ground state spectrum. The resulting amplitudes were used to determine the excited state fraction. For the spectrum shown in Figure 4, the fraction was found to be $(63 \pm 2)\%$. This value is larger by a factor of 1.7 than that obtained in previous measurements with the same concentration and laser fluence.[29,32] This difference is attributed to the use of the microfocused x-ray beam. Because the x-rays were focused to a spot size smaller than the laser spot size, only those molecules in the laser focus volume that see the highest fluence are probed. This effectively increases the rate at which data from excited state molecules are collected and indicates that addition of the microprobe could improve acquisition times even for kHz experiments.

Figure 5 shows the ratio of the singlet laser-on and laser-off counts as a function of the delay between the x-ray and laser pulses while the x-ray photon energy was kept fixed at the $1s \rightarrow 4p_z$ resonance in the T_1 laser excited state (8.34 keV). The scan took 15 min. Each point was integrated for 20 s. The excited state decay can be approximated by a single exponential decay for the T_1 state, since the two intermediate states have short lifetimes (<350 fs and <20 ps) compared to the 200 ps lifetime of the T_1 state. The time over which the laser excitation occurs can be neglected since the laser pulse duration is short (10 ps FWHM) relative to the x-ray pulse duration (94 ps FWHM). The observed signal can then be fit with a convolution of a 94 ps FWHM Gaussian and an exponential decay. The extracted lifetime of the T_1 state was found to be (186 ± 10) ps, in agreement with previous results.[29] The peak in the on/off ratio occurs 50 ps after "time-zero", the
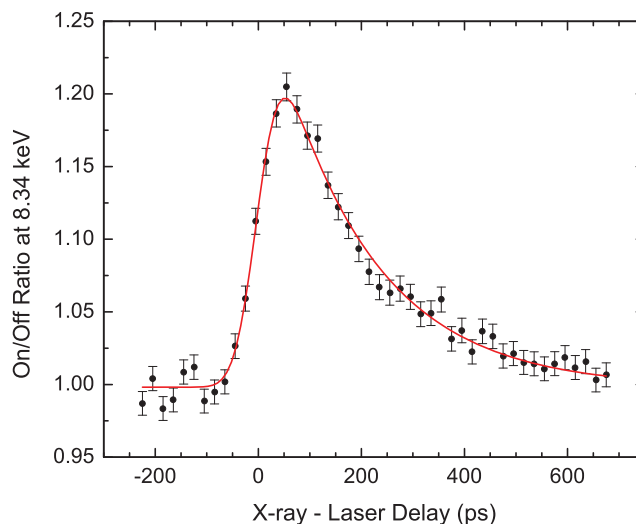

FIG. 5. (Color online) Time evolution of the $1s \rightarrow 4p_z$ resonance of the T_1 laser excited state of NiTMP (8.34 keV). The ratio of the singlet laser-on and laser-off counts is plotted. The solid line is a fit of a Gaussian function (accounting for the 94 ps FWHM x-ray pulse) convolved with an exponential decay function. The fit gives a decay time of 186 ± 10 ps for the T_1 state. The data were collected at 135.8 kHz and the laser power was 0.7 W.
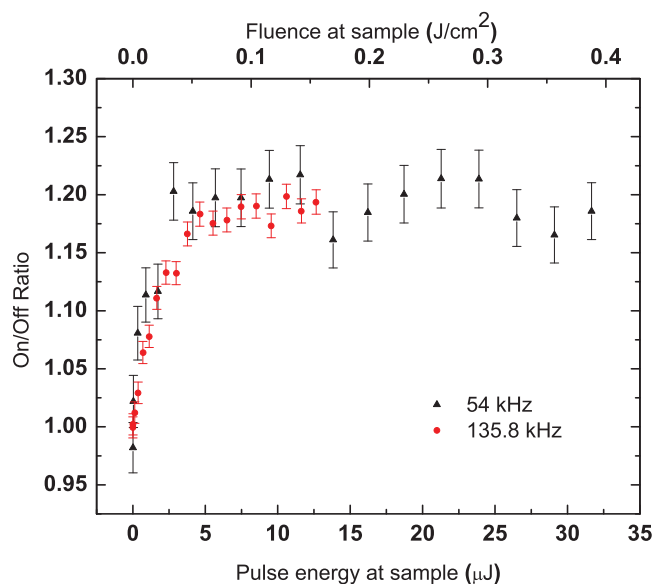
FIG. 6. (Color online) Laser-on/laser-off ratio at the $1s \rightarrow 4p_z$ resonance of the T_1 laser excited state of NiTMP (8.34 keV) as a function of the laser fluence. The laser was focused to a FWHM spot size of 60×60 μm^2.

FIG. 7. (Color online) Normalized absorption coefficient, μ, as a function of x-ray energy for the pre-edge $1s \rightarrow 3d$ features of the ground and excited states of NiTMP in solution. The extracted excited state spectrum (open circles) was fit (solid line) to a sum of two Gaussians (dashed) and an arctangent (dashed) background. The Gaussian fits to the $3d_{x^2-y^2}$ (8.3339 keV) and $3d_{z^2}$ (8.3315 keV) resonances show a splitting of 2.4 eV. The ground state spectrum (filled circles and line) with a $3d_{x^2-y^2}$ single peak at 8.3330 keV is shown for comparison. The Gaussian plots are offset by .01 for clarity. The data was collected at 135.8 kHz. The x-rays probed 50 ps after the laser excitation. The laser power was 0.7 W.

delay at which the peak of the laser pulse is centered within the x-ray pulse envelope. The 50 ps delay is as expected for a 100 ps x-ray pulse. The spectra in Figure 4 were taken at this peak delay.

The on/off ratio at the $1s \rightarrow 4p_z$ resonance was also observed as a function of the laser fluence. Two scans, at 54.3 kHz and 135.8 kHz, are shown in Figure 6. The power at the sample was reduced using an attenuator comprised of a half-waveplate and polarizer. The scans took ∼5 min to collect and show a saturation in the fluorescence yield at a laser energy of about 6 μJ per pulse with a laser focal spot of 60 μm × 60 μm. This corresponds to roughly 2×10^{19} photons/cm^3. Given the NiTMP number density of 1.2×10^{18} /cm^3, this is about 15 photons for each molecule within the probed region.

The ability to collect data faster is particularly important when studying subtle effects. Figure 7 shows the ground and laser excited absorption spectra in the pre-edge region near the $1s \rightarrow 3d$ resonances. Since these transitions are dipole-forbidden (but quadrupole-allowed), their strength is very weak. However, they are of great interest because they involve the unoccupied metal-centered molecular orbitals which are important for the properties of the excited state metalloporphyrin molecules, such as energy transfer, electron shifting, and spin-orbit coupling, and so contain a great deal of information about the electronic configurations of states and excited state decay pathways. Because in the ground state all d orbitals are filled except for the $3d_{x^2-y^2}$, only one transition to the unoccupied $3d_{x^2-y^2}$ state is seen in the pre-edge region in the ground state spectrum. In the T_1 excited state, the $3d_{x^2-y^2}$ and $3d_{z^2}$ orbitals are half filled. The excited state spectrum, which has been treated here so that the ground state component is removed, clearly shows two peaks, attributed to transitions to these half vacant orbitals in the T_1 state. These spectra, covering the $3d$ resonance region, took 50 min to collect, averaging 30 s per point which can be compared to previ-
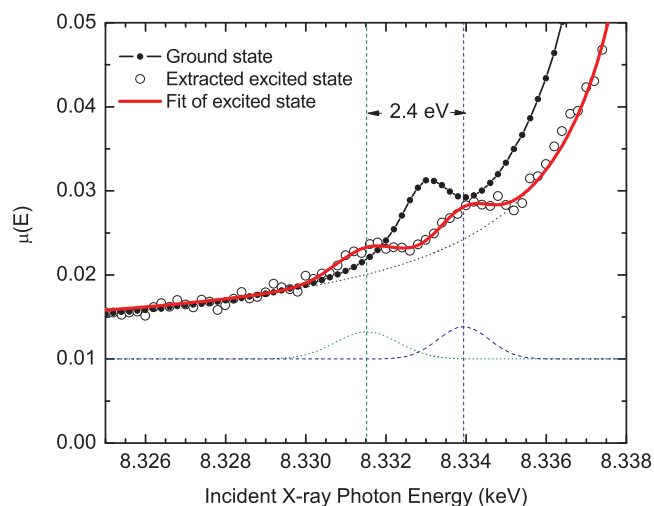
ous, somewhat inferior, results collected with 400 s averaging using a 1 kHz pump-probe repetition rate.[29]

V. SUMMARY AND OUTLOOK

By combining a high repetition rate amplified laser system as a pump source and microfocused hard x-rays as a probe source, we have shown that time-resolved x-ray absorption spectroscopy data can be collected much more efficiently than in previous studies. Utilizing a higher fraction of the available x-ray flux of the synchrotron allows for the collection of higher quality data and opens up the possibility of studying dilute samples that were previously inaccessible. The high repetition rate pump-probe scheme also enables the use of sensitive, but x-ray flux demanding, measurements such as x-ray emission spectroscopy and x-ray diffuse scattering. An important aspect of the high repetition rate laser system is its ability to run at a range of repetition rates providing flexibility to adapt to the filling pattern of the synchrotron as well as to the needs of a particular experiment. For example, while not a major limitation for the present experiment due to the fast decay of the NiTMP T_1 state, for samples with long-lived laser-excited states, relative to the time between laser pulses, the flow rate of the liquid jet will need to be fast enough to ensure that the pumped molecules have vacated the interaction region by the next laser pump pulse. Our liquid pump can generate flows with speeds of ∼15 m/s. With a laser focus spot of 25 μm FWHM this would enable the use of ∼1 MHz repetition rates. A slower flow rate may be more suitable for some samples, however, and the laser can accommodate this.

The present demonstration experiment was run at a repetition rate of 135.8 kHz. However, it is clear that we can

saturate optical excitations with smaller than the maximum available fluence, and hence run at even higher repetition rates. Very recent experiments have been carried out on different molecular systems at repetition rates of 1.3 MHz and 3.25 MHz, efficiently using the full flux of the APS. The high repetition rates enabled simultaneous collection of x-ray absorption, high resolution x-ray emission, and x-ray diffuse scattering data. These scientific results will be reported elsewhere.[33]

While the temporal resolution of synchrotron sources is presently limited, due to the long x-ray pulse duration, an upgrade of the Advanced Photon Source is planned that would reduce the pulse duration to ~1 ps while maintaining high brightness and high repetition rate.[34,35] High repetition rate methods will play an important role in utilizing this new source.

ACKNOWLEDGMENTS

[1]M. Chergui and A. Zewail, ChemPhysChem **10**, 28 (2009).
[2]L. X. Chen, Angew. Chem., Int. Ed. **43**, 2886 (2004).
[3]L. X. Chen, Annu. Rev. Phys. Chem. **56**, 221 (2005).
[4]C. Bressler and M. Chergui, Chem. Rev. **104**, 1781 (2004).
[5]T. Pfeifer, C. Spielmann, and G. Gerber, Rep. Prog. Phys. **69**, 443 (2006).
[6]R. Santra, R. W. Dunford, E. P. Kanter, B. Krässig, S. H. Southworth, and L. Young, Adv. At., Mol., Opt. Phys. **56**, 219 (2008).
[7]R. Santra, J. Phys. B **42**, 023001 (2009).
[8]A. Ravasio, D. Gauthier, F. R.N.C. Maia, M. Billon, J.-P. Caumes, D. Garzella, M. Géléoc, O. Gobert, J.-F. Hergott, A.-M. Pena, H. Perez, B. Carré, E. Bourhis, J. Gierak, A. Madouri, D. Mailly, B. Schiedt, M. Fajardo, J. Gautier, P. Zeitoun, P. H. Bucksbaum, J. Hajdu, and H. Merdji, Phys. Rev. Lett. **103**, 028104 (2009).
[9]R. L. Sandberg, D. A. Raymondson, C. La-O-Vorakiat, A. Paul, K. S. Raines, J. Miao, M. M. Murnane, H. C. Kapteyn, and W. F. Schlotter, Opt. Lett. **34**, 1618 (2009).
[10]T. Popmintchev, M. C. Chen, A. Bahabad, M. Gerrity, P. Sidorenko, O. Cohen, I. P. Christov, M. M. Murnane, and H. C. Kapteyn, PNAS **106**, 10516 (2009).
[11]S. Kneip, C. McGuffey, J. L. Martins, S. F. Martins, C. Bellei, V. Chvykov, F. Dollar, R. Fonseca, C. Huntington, G. Kalintchenko, A. Maksimchuk, S. P.D. Mangles, T. Matsuoka, S. R. Nagel, C. A.J. Palmer, J. Schreiber, K. T. Phuoc, A. G.R. Thomas, V. Yanovsky, L. O. Silva, K. Krushelnick, and Z. Najmudin, Nat. Phys. **6**, 980 (2010).
[12]A. Rousse, K. T. Phuoc, R. Shah, A. Pukhov, E. Lefebvre, V. Malka, S. Kiselev, F. Burgy, J.-P. Rousseau, D. Umstadter, and D. Hulin, Phys. Rev. Lett. **93** (2004).
[13]N. Zhavoronkov, Y. Gritsai, M. Bargheer, M. Woerner, and T. Elsaesser, Appl. Phys. Lett. **86**, 244107 (2009).
[14]C. Reich, C. M. Laperle, X. Li, B. Ahr, F. Benesch, and C. G. Rose-Petruck, Opt. Lett. **32**, 427 (2007).
[15]B. W. J. McNeil and N. R. Thompson, Nature Photon. **4**, 814 (2010).
[16]D. H. Bilderback, P. Elleaume, and E. Weckert, J. Phys. B **38**, S773 (2005).
[17]E. A. Stern, D. L. Brewe, K. M. Beck, S. M. Heald, and Y. Feng, Phys. Scr. **2005**, 1044 (2005).
[18]P. Fons, A. V. Kolobov, T. Fukaya, M. Suzuki, T. Uruga, N. Kawamura, M. Takagaki, H. Ohsawa, H. Tanida, and J. Tominaga, Jpn. J. Appl. Phys. **46**, 3711 (2007).
[19]E. M. Dufresne, B. Adams, M. Chollet, R. Harder, Y. Li, H. Wen, S. J. Leake, L. Beitra, X. Huang, and I. K. Robinson, "A technique for high-frequency laser-pump x-ray probe experiments at the aps," Nucl. Instrum. Methods Phys. Res. A (in press).
[20]E. R. Peterson, C. Buth, D. A. Arms, R. W. Dunford, E. P. Kanter, B. Krässig, E. C. Landahl, S. T. Pratt, R. Santra, S. H. Southworth, and L. Young, Appl. Phys. Lett. **92**, 094106 (2008).
[21]T. E. Glover, M. P. Hertlein, S. H. Southworth, T. K. Allison, J. van Tilborg, E. P. Kanter, B. Krässig, H. R. Varma, B. Rude, R. Santra, A. Belkacem, and L. Young, Nat. Phys. **6**, 69 (2009).
[22]L. Young, D. A. Arms, E. M. Dufresne, R. W. Dunford, D. L. Ederer, C. Höhr, E. P. Kanter, B. Krässig, E. C. Landahl, E. R. Peterson, R. Rudati, R. Santra, and S. H. Southworth, Phys. Rev. Lett. **97**, 83601 (2006).
[23]B. Krassig, R. W. Dunford, E. P. Kanter, E. C. Landahl, S. H. Southworth, and L. Young, Appl. Phys. Lett. **94**, 171113 (2009).
[24]E. M. Dufresne, B. Adams, D. A. Arms, M. Chollet, E. C. Landahl, Y. Li, D. A. Walko, and J. Wang, AIP Conf. Proc. **1234**, 181 (2010).
[25]P. J. Eng, M. Newville, M. L. Rivers, and S. R. Sutton, Proc. SPIE **3449**, 145 (1998).
[26]L. X. Chen, W. J. H. Jager, G. Jennings, D. J. Gosztola, A. Munkholm, and J. P. Hessler, Science **292**, 262 (2001).
[27]M. Saes, C. Bressler, R. Abela, D. Grolimund, S. L. Johnson, P. A. Heimann, and M. Chergui, Phys. Rev. Lett. **90**, 47403 (2003).
[28]M. Khalil, M. A. Marcus, A. L. Smeigh, J. K. McCusker, H. H. W. Chong, and R. W. Schoenlein, J. Phys. Chem. A **110**, 38 (2006).
[29]L. X. Chen, X. Zhang, E. C. Wasinger, K. Attenkofer, G. Jennings, A. Z. Muresan, and J. S. Lindsey, J. Am. Chem. Soc. **129**, 9616 (2007).
[30]X. Zhang, E. C. Wasinger, A. Z. Muresan, K. Attenkofer, G. Jennings, J. S. Lindsey, and L. X. Chen, J. Phys. Chem. A **111**, 11736 (2007).
[31]S. Della-Longa, L. X. Chen, P. Frank, K. Hayakawa, K. Hatada, and M. Benfatto, Inorg. Chem. **48**, 3934 (2009).
[32]L. X. Chen, X. Zhang, E. C. Wasinger, J. V. Lockard, A. B. Stickrath, M. W. Mara, K. Attenkofer, G. Jennings, G. Smolentsev, and A. Soldatov, Chem. Sci. **1**, 642 (2010).
[33]A. Bordage, C. Bressler, S. E. Canton, G. Doumy, R. W. Dunford, A. Galler, W. Gawelda, K. Haldrup, E. P. Kanter, K. S. Kjaer, H. T. Lemke, A. M. March, M. M. Nielsen, D. Ray, S. H. Southworth, J. Uhlig, T. Van Driel, G. Vanko, and L. Young (unpublished).
[34]A. Zholents, P. Heimann, M. Zolotorev, and J. Byrd, Nucl. Instrum Methods Phys. Res. A, **425**, 385 (1999).
[35]M. Borland, Phys. Rev. ST Accel. Beams **8**, 74001 (2005).